Near-threshold Fatigue Crack Behavior of Thin Copper Sheet and its Application for Structural Health Monitoring

Takayuki Shiraiwa[1,*], **Manabu Enoki**[1]

[1] Department of Materials Engineering, The University of Tokyo, Tokyo 113-8656, Japan
* Corresponding author: shiraiwa@rme.mm.t.u-tokyo.ac.jp

Abstract Smart stress-memory patch is a novel sensing method in structural health monitoring for evaluating fatigue damage. The patch can estimate the number of cycles and stress amplitude using fatigue crack growth properties in Paris region of thin metal sheets. In this study, near-threshold fatigue crack growth behavior in thin pure copper sheet was investigated under strain-controlled testing to improve the measuring range and accuracy. Using a function describing the initiation as well as the stable growth of fatigue cracks, the relationship between stress intensity factor range and crack growth rate was successfully fitted to one equation regardless of strain amplitude. Based on these experimental results, a new equation for estimating fatigue cycles and stress amplitude from fatigue crack length of two specimens was derived. This equation overcame the limitation that the patch requires two or more materials with different fatigue characteristics. The new equation needs only one material for simultaneous estimation of fatigue cycles and stress amplitude, and the measuring range can be controlled by geometry of specimen. Since this patch needs neither power supply nor wiring, it provides a great potential for long-term structural health monitoring with easy maintenance and low cost.

Keywords Fatigue crack growth, Finite element method, Copper, Structural health monitoring, Smart stress-memory patch

1. Introduction

Structural health monitoring (SHM) is highly required to ensure the reliability of bridges, ships, trains, aircraft, power plants and industrial machines. Especially, a long-term sensing method of fatigue damage is very important to avoid the fracture caused by cyclic loading. Strain gauge, FBG (Fiber Bragg Grating) sensor and wireless strain sensing systems are utilized to monitor strain and to evaluate fatigue damage. However, there are several problems on the practical use such as necessity of wiring, electrical power supply and complicated measuring devices. Concept of smart stress-memory patch (hereinafter called "smart patch") was proposed to overcome above problems in the previous papers [1-6]. Sensor in smart patch consists of a thin metal sheet with a pre-crack, and the number of fatigue cycles and stress amplitude on structure can be estimated from fatigue crack growth in the sensor. Smart patch is a promising technique for long-term SHM because it needs neither power supply nor wiring. Furthermore, the patch is successfully applied to batteryless wireless system to measure the crack length in the sensor using RFID [4].

The fatigue crack growth behavior in the sensor under stress-controlled fatigue test has been investigated to estimate stress amplitude and fatigue cycles [1, 2]. However, when the patch is attached to structure, the sensor is subjected to strain-controlled loading under the change in strain of the structure. Therefore, it is necessary to evaluate fatigue behavior in the sensor under strain-controlled conditions for application of smart patch to structure. While most studies about fatigue in thin metal sheet have focused on stress-life (S-N) and strain-life (ε-N) curves for reliability of microelectronic products [7-10], the fatigue crack growth behavior under strain-controlled testing has not been enough explored in detail.

In this study, fatigue crack growth behavior of the sensor (thin pure copper sheet) was evaluated under uniaxial strain-controlled fatigue testing in order to obtain the characteristics of the attached sensor to structure. The scattering in crack growth was also examined by a stochastic model to assess the error in estimation of fatigue cycles and stress amplitude. From these observations, a method to evaluate fatigue cycles and residual fatigue life of structure using smart patch was proposed.

2. Principle of smart stress-memory patch

The details of the principle were described in the previous paper [5]. A schematic image is shown in Fig. 1 (a). Sensor in the patch consists of a thin metal sheet with a pre-crack. Since fatigue damage in structure tends to occur in structural component, more than one sensor is attached, for example, close to the welded part. When the structure is subjected to cyclic loading, the sensor is also cyclically loaded in response to the change of strain in the structure. Then, fatigue crack growth from pre-crack in the sensor will occur according to the cyclic loading. After a certain period, the crack length in each sensor will be measured by optical microscope or wireless measurement of electrical resistance change. The number of fatigue cycles (N) and stress amplitude ($\Delta\sigma$) on the structure can be estimated from the crack length detected from two sensors with different characteristics as shown in Fig. 1 (b).

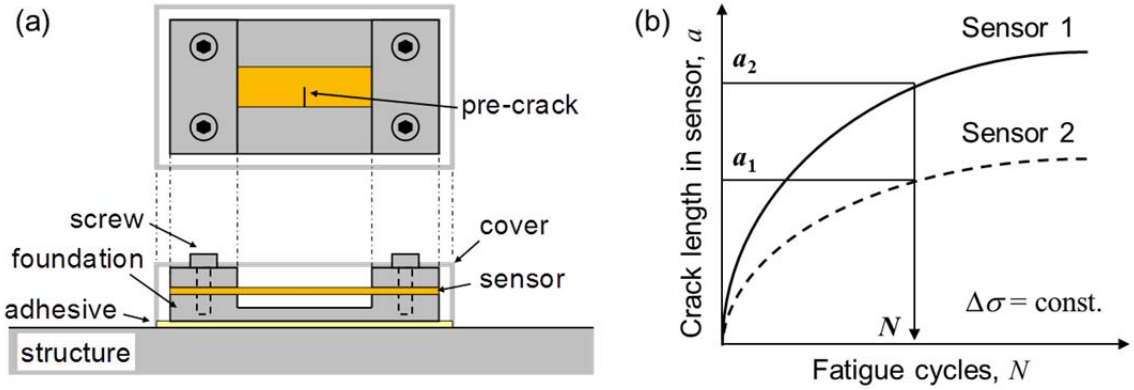

Figure 1. (a) Schematic image of smart stress-memory patch and (b) principle to estimate cyclic number from crack length.

3. Experimental procedure

3.1. Materials

The sensors were made of electrodeposited (ED) copper and nickel. These electrodeposited materials tend to have a very small grain size and provides stable crack propagations [11, 12]. The ED-Cu sheet with a thickness of 0.1 mm was cut to rectangular coupons with a dimension of 40 mm × 5 mm, 40 mm × 10 mm and 60 mm × 10 mm, and the ED-Ni sheet with a thickness of 0.05 mm was cut to 40 mm × 5 mm. Specimen geometries are shown in Fig. 2. A single notch with a length of 2.5 mm and a width of 0.3 mm was induced at the center from one side of the coupon. The notch tip was a round-shaped with a radius of approximately 150 μm. Additionally, the notch tip was sharpened to curvature radius of about 30 μm by the blade (High-stainless 100 μm, Feather Safety Razor Co., Ltd.). One side of the coupon was polished to a mirror finish using 3 μm and 1 μm alumina slurry to observe crack length clearly. Afterward, fatigue pre-crack was introduced.

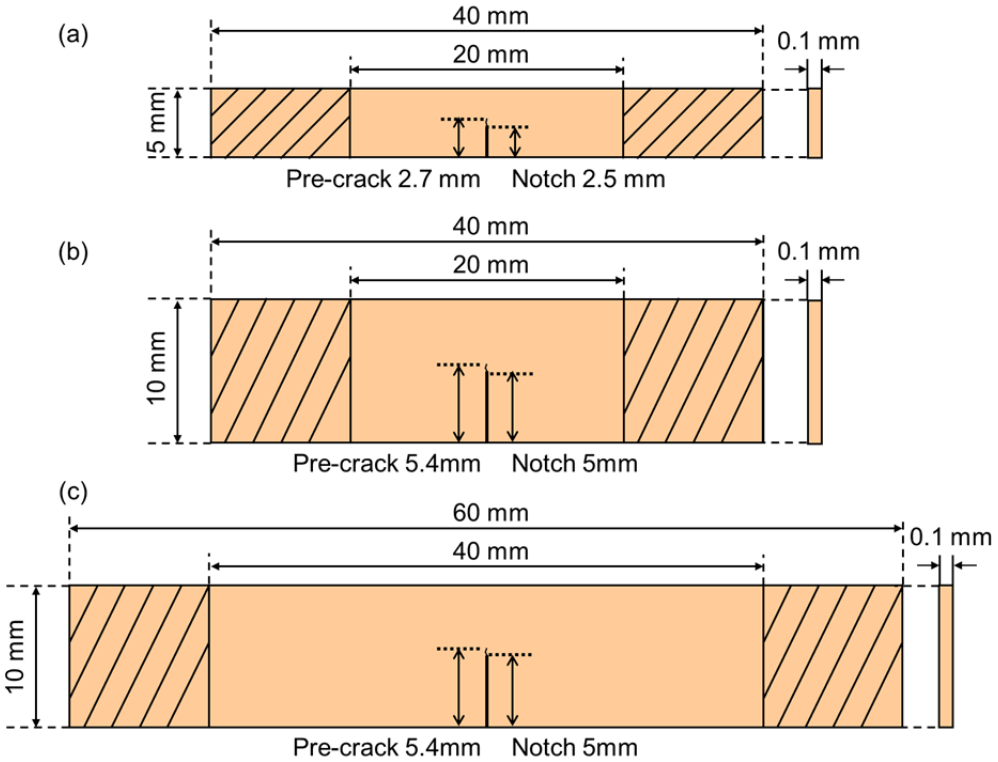

Figure 2. Specimen geometry. (a) Standard type, (b) High-cycle type, (c) High-sensitive type.

3.2. Fatigue test

Both ends of the sensor were clamped in jigs mounted in a fatigue testing machine (MMT-100N, Shimadzu), and the gauge length between the upper and lower jigs is adjusted to 20 mm. Fatigue tests were performed under maximum crosshead displacement (u_{max}) of 20, 25 and 30 μm, displacement ratio of R = 0.1 to 0.5, and frequency of 19 Hz. The strain ratio (R) was 0.1 and maximum strain (ε_{max}) was changed from 0.05 to 0.2 % where the strain is defined as a crosshead displacement divided by gauge length of specimen. The crack length was measured optically with digital microscope (VHX-600, Keyence).

3.3 Stress intensity factor

A proper shape factor, $f(\alpha)$, for the present sensor geometry is necessary to characterize the fatigue crack growth behavior as a function of stress intensity factor range, ΔK. It is commonly known that the stress intensity factor of single edge-cracked tension specimen with prescribed end displacements can be expressed by

$$K = \sigma\sqrt{\pi a}\cdot f(\alpha,\beta),\quad \sigma = \frac{Eu}{L},\quad \alpha = \frac{a}{W},\quad \beta = \frac{L}{W}, \tag{1}$$

where W is width of the specimen, L is gauge length of the specimen, a is crack length, E is Young's modulus, u is displacement on the specimen, α is normalized crack length and β is ratio of the gauge length to the width. Although the shape factor has been investigated in the range of β = 0.5 to 1 [13], the present sensor has the higher value of β = 2.0 to 4.0.

In order to evaluate shape factor of the sensor, linear elastic stress analysis was performed by finite element method (FEM). Geometry and boundary conditions for the simulation are shown in Fig. 3 (a), where Young's modulus was 120 GPa, Poisson ratio was 0.34 and L, W and u was changed as the same as experimental conditions. The model was sectioned into quadrilateral plane stress elements

with size of 0.05 mm × 0.05 mm. In the analysis, ten integration paths were defined from the crack tip to the outside, and the *J*-integral was calculated for normalized crack length ($\alpha = a/W$) ranging from 0.1 to 0.9. Since the *J*-integral reached a constant value from the fifth path in each condition, the constant value was used for calculation of stress intensity factor. Under plane stress conditions, the stress intensity factor can be described by

$$J = K^2/E, \tag{2}$$

and the shape factor was solved using eq. (1) and (2) as a function of stress intensity factor range, as shown in Fig. 3(b). The shape factors can be fitted as follows:

$$f(\alpha) = 1.002 - 0.040\alpha - 1.52\alpha^2 + 1.09\alpha^3 \quad (\beta = 2), \tag{3}$$

$$f(\alpha) = 0.896 - 1.43\alpha - 2.71\alpha^2 + 1.02\alpha^3 \quad (\beta = 4), \tag{4}$$

The calculated shape factor of β = 0.5 to 1 showed good agreement with the results by boundary element method (BEM) [13].

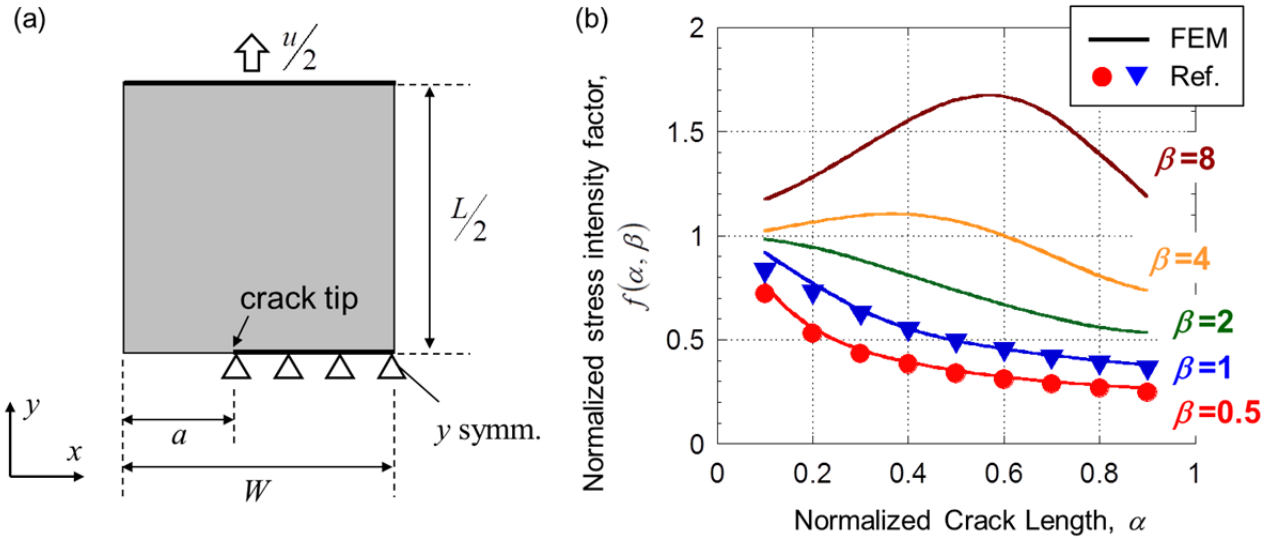

Figure 3. (a) Rectangular plate with prescribed end displacement, (b) Normalized stress intensity factor under plane stress condition.

4. Results

4.1. Fatigue crack growth behavior of ED-Cu

Near-threshold fatigue crack growth behavior in thin pure copper sheet with pre-crack was evaluated under strain-controlled fatigue testing. Fatigue crack path of the sensor exhibited the significantly straight line as shown in Fig. 4 (a). The relationships between the crack growth rate and stress intensity factor range is shown in Fig. 4 (b). The fit curve was analyzed by the following Kohout equation[14]:

$$\frac{da}{dN} = C\left[\left\{\frac{\Delta K}{(1-R)^{1-\beta_w}}\right\}^m - \Delta K_{th0}^m\right] \tag{5}$$

where, C, m, β_w are material constants and ΔK_{th0} is the threshold value of stress intensity factor range with R = 0. The fit is relatively good and the calculated values of the parameters are $C = 1.16 \times 10^{-11}$, m = 2.87, ΔK_{th0} = 4.41 MPa·m$^{1/2}$, β_w = 0.198.

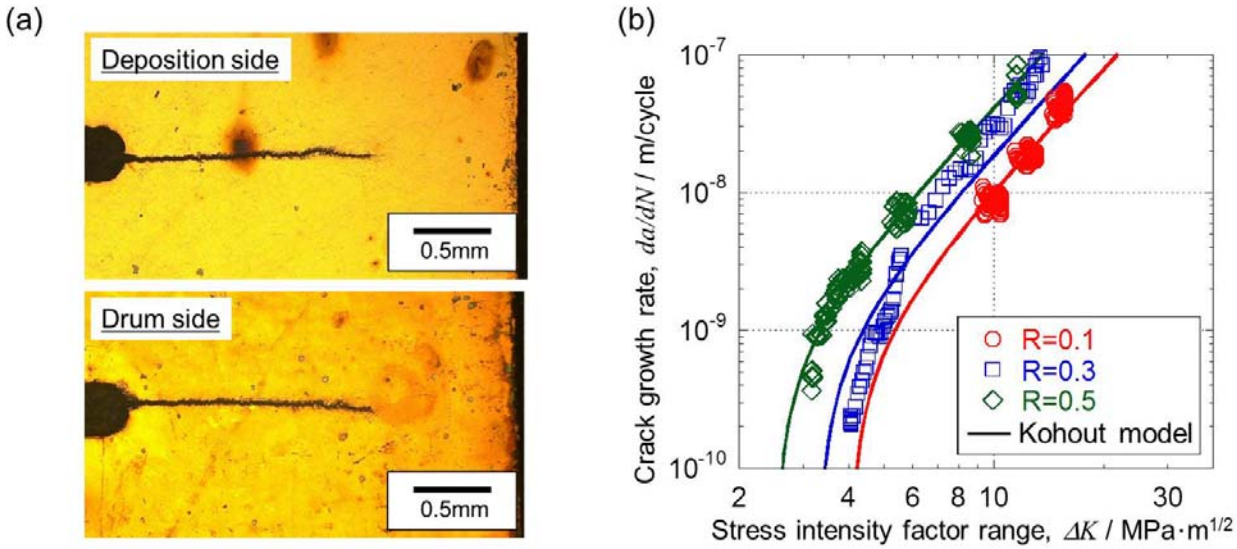

Figure 4. (a) Fatigue crack path of ED-Cu sheet. (b) Relationship between stress intensity factor range calculated from FEM and experimental crack growth rate.

4.2. Fatigue crack growth behavior of ED-Ni

Fatigue tests with ED-Ni were also performed to obtain the sensor characteristics of smart patch. The fatigue crack path observed from the drum side was smooth while the opposite side was relatively rough. The fatigue crack growth behavior of ED-Ni is shown in Fig 5 (b). The experimental results were within Paris region and the effect of strain ration was observed. Therefore, the fit curve was analyzed by the Walker equation:

$$\frac{da}{dN} = C\left[\frac{\Delta K}{(1-R)^{1-\beta_W}}\right]^m \tag{6}$$

The calculated parameters were m =3.26, C =4.54×10^{-12}, β_w =0.556.

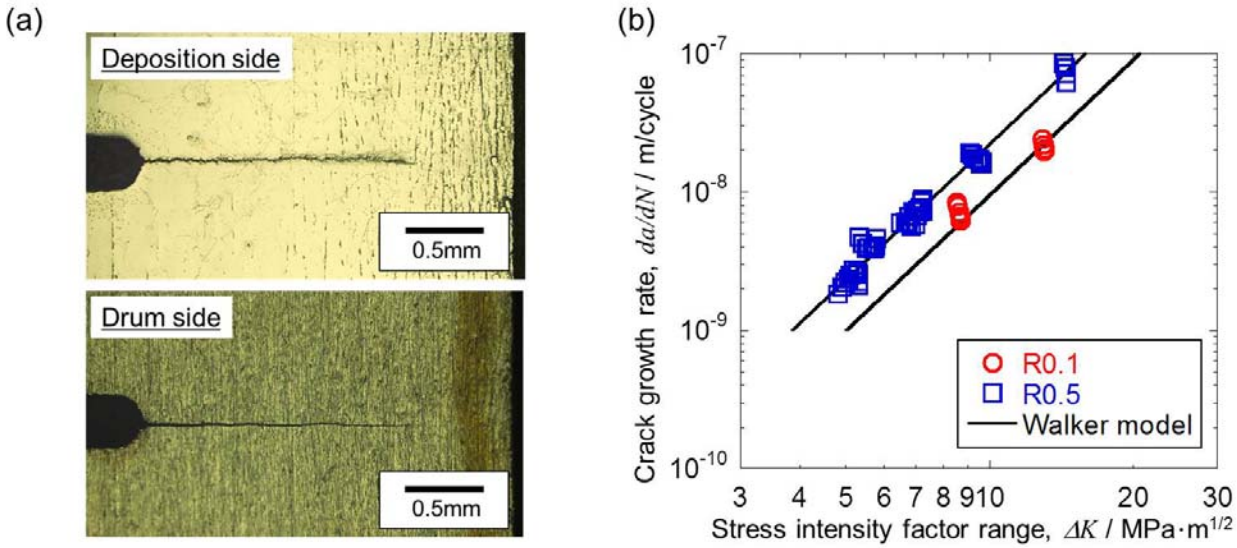

Figure 5. (a) Fatigue crack path of the ED-Ni sheet. (b) Relationship between stress intensity factor range and fatigue crack growth rate in ED-Ni specimen.

4.3. Effect of specimen geometry on fatigue crack growth

Three different specimen geometries were used in the present study. All specimens were made of ED-Cu. The fatigue crack growth rate is shown in Fig. 6 (a). The relationship between stress intensity factor range calculated from FEM and experimental crack growth rate is fitted on one curve regardless of the geometries as shown in Fig. 6 (b).

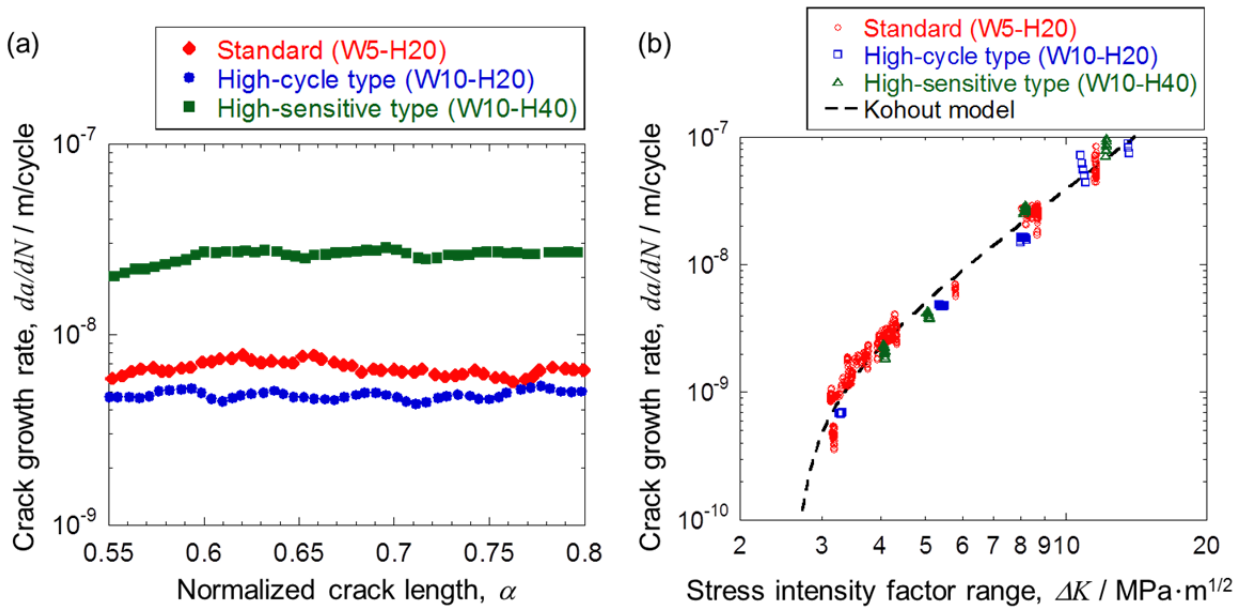

Figure 6. (a) Fatigue crack growth rate of ED-Cu specimens with three geometries. (b) Relationship between stress intensity factor range and fatigue crack growth rate of ED-Cu specimens with three geometries.

5. Discussion

5.1. Fatigue crack growth behavior

Many studies about fatigue behavior in thin metal sheet have shown that fatigue life is associated with the grain structure and specimen thickness using smooth specimen [7-10]. In the present study, fatigue crack propagation experiments were performed with notched specimen under strain-controlled condition. The crack path of the specimen exhibited almost straight line as shown in Fig. 4 (a) and Fig. 5. (a). It allows us to measure the crack length in the sensor easily. Among them, the path observed from the deposition side in ED-Ni was relatively rough due to the development of columnar grains during electrodepositing process. The relationship between stress intensity factor range calculated from FEM and experimental crack growth rate is fitted to one equation regardless of strain amplitude, strain ratio and specimen geometry. Therefore, two specimens made of different materials are needed to apply the principle of smart stress-memory patch. The threshold value of stress intensity factor range was determined by Kohout equation, which is related to the minimum value of detectable stress amplitude.

5.2. Estimation of fatigue damage using two materials

Based on fatigue testing results, a method to evaluate fatigue damage of structure using smart patch will be discussed. When the patch is attached to structure, the sensor is subjected to strain-controlled loading under the change in strain of the structure. A simple model for the attached sensor to structure is depicted in Fig. 7. It is assumed that the far-field stress in the plate is a uniaxial tension ($\sigma_{structure}$) in

elastic region and the sensor is perfectly bonded on the plate. If thickness of the sensor is enough thin, strain distribution in the plate is uniform regardless of the presence of the sensor, and $\sigma_{structure}$ is described as follows:

$$\sigma_{\text{structure}} = E_{\text{strucutre}} \frac{u}{L}, \tag{7}$$

where $E_{\text{strucuture}}$ is Young's modulus of structure, u is the displacement on the sensor and L is gauge length of the sensor, respectively. Using Walker equation, the fatigue cycles, N, is represented as the function of the normalized crack length, α, and the maximum strain, $\varepsilon_{\max}$, as:

$$N = \frac{W_2}{C_2}\left\{E_2\varepsilon_{\max}(1-R)^{\beta_{W2}}\sqrt{\pi W_2}\right\}^{-m_2}\int_{\alpha_{0,2}}^{\alpha_2}\left\{\sqrt{\alpha}f(\alpha)\right\}^{-m2}\mathrm{d}\alpha. \tag{8}$$

Furthermore, when two sensors of different properties are employed, simultaneous equation are given as follows,

$$N = \frac{W}{C_1}\left\{E_1\varepsilon_{\max}(1-R)^{\beta_{W1}}\sqrt{\pi W_1}\right\}^{-m_1}\int_{\alpha_{0,1}}^{\alpha_1}\left\{\sqrt{\alpha}f(\alpha)\right\}^{-m_1}\mathrm{d}\alpha,$$

$$N = \frac{W_2}{C_2}\left\{E_2\varepsilon_{\max}(1-R)^{\beta_{W2}}\sqrt{\pi W_2}\right\}^{-m_2}\int_{\alpha_{0,2}}^{\alpha_2}\left\{\sqrt{\alpha}f(\alpha)\right\}^{-m2}\mathrm{d}\alpha. \tag{9}$$

Indexes 1 and 2 represent sensor 1 and 2, respectively. From these equations, the fatigue cycles and the stress amplitude of structure, $\sigma_{\text{strucuture}}$, are obtained as:

$$N = \left[\frac{{C_2}^{m_1}}{{C_1}^{m_2}}\cdot\frac{{W_1}^{m_2}}{{W_2}^{m_1}}\cdot\left\{(1-R)^{\beta_{W2}-\beta_{W1}}\frac{E_2}{E_1}\sqrt{\frac{W_2}{W_1}}\right\}^{m_1m_2}\cdot\frac{F_1(\alpha_1)}{F_2(\alpha_2)}\right]^{\frac{1}{m_2-m_1}},$$

$$\Delta\sigma_{\text{structure}} = E_{\text{structure}}(1-R)\left[\frac{C_2}{C_1}\cdot\frac{W_1}{W_2}\cdot\frac{\left\{E_2(1-R)^{\beta_{W2}}\sqrt{\pi W_2}\right\}^{m_2}}{\left\{E_1(1-R)^{\beta_{W1}}\sqrt{\pi W_1}\right\}^{m_1}}\cdot\frac{F_1(\alpha_1)}{F_2(\alpha_2)}\right]^{\frac{1}{m_1-m_2}}. \tag{10}$$

In the case that the steel structure ($E_{\text{strucuture}}$ = 200 GPa) is subjected to cyclic loading with the stress ratio of 0.1, the fatigue cycles and the stress amplitude were calculated by eqs. (10) and experimental parameters of ED-Cu and ED-Ni, as shown in Fig. 8. Stress amplitude can be estimated from crack length detected from two sensors with different characteristics. Therefore, it was shown that fatigue cycles on structures can be estimated using smart patch.

Evaluation of fatigue damage of structure is important to avoid the rapture caused by cyclic loading. Cumulative fatigue damage is commonly determined using the Palmgren-Miner rule [15]. In this rule, the amount of fatigue damage, D, is given as the ratio of cyclic number of N / N_{f}, where N_{f} is the number of cycles to failure. Based on many studies about fatigue life of structural components, relationship between stress amplitude and the number of cycles to failure is generally characterized by S-N curve in high-cycle fatigue situations as:

$$N_f = C_{SN}\Delta\sigma^{-m_{SN}}, \tag{11}$$

where C_{SN} and m_{SN} is material constants and $\Delta\sigma$ is stress amplitude [16]. Using the fatigue cycles calculated by smart patch and S-N curve (as shown in Fig. 9(a)), the amount of fatigue damage can be evaluated as shown in Fig. 9 (b). Therefore, it was demonstrated that the health of structure can be estimated using smart patch.

5.3. Estimation of fatigue damage using single material

Another equation for estimating fatigue cycles and stress amplitude from fatigue crack length of two specimens can be derived using near-threshold fatigue crack behavior as shown in Fig. 10. Using Kohout equation, the fatigue cycles, N, is represented as:

$$N = \frac{W_1}{C}\int_{\alpha_0}^{\alpha_1}\left[\frac{d\alpha}{\left\{\varepsilon_{\max}E(1-R)^{\beta_w}\sqrt{\pi W\alpha}\,f_1(\alpha)\right\}^m - \Delta K_{th0}{}^m}\right]. \tag{11}$$

This equation overcame the limitation that the patch requires two or more materials with different fatigue characteristics. Estimation map of fatigue cycles and stress amplitude of steel structure as a function of normalized crack length in two sensors made of same material are shown in Fig. 11. The new equation needs only one material for simultaneous estimation of fatigue cycles and stress amplitude, and the measuring range can be controlled by geometry of specimen. Since this patch needs neither power supply nor wiring, it provides a great potential for long-term structural health monitoring with easy maintenance and low cost.

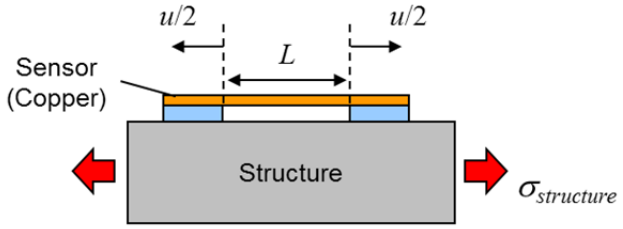

Figure 7. Schematic of simple model for the attached sensor to structure.

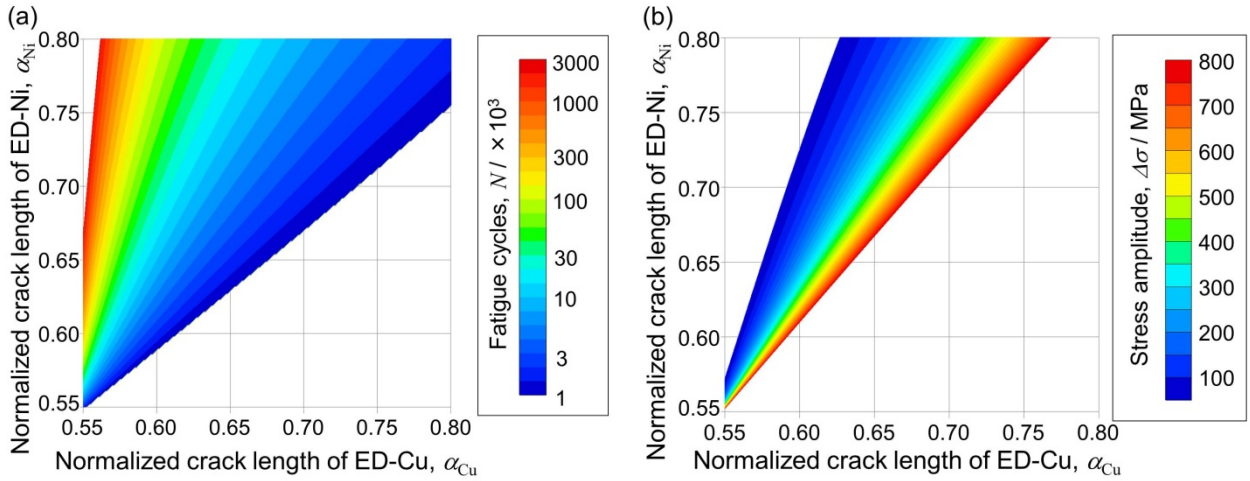

Figure 8. Estimation map of (a) fatigue cycles and (b) stress amplitude of steel structure as a function of normalized crack length in two sensors consisted of different materials.

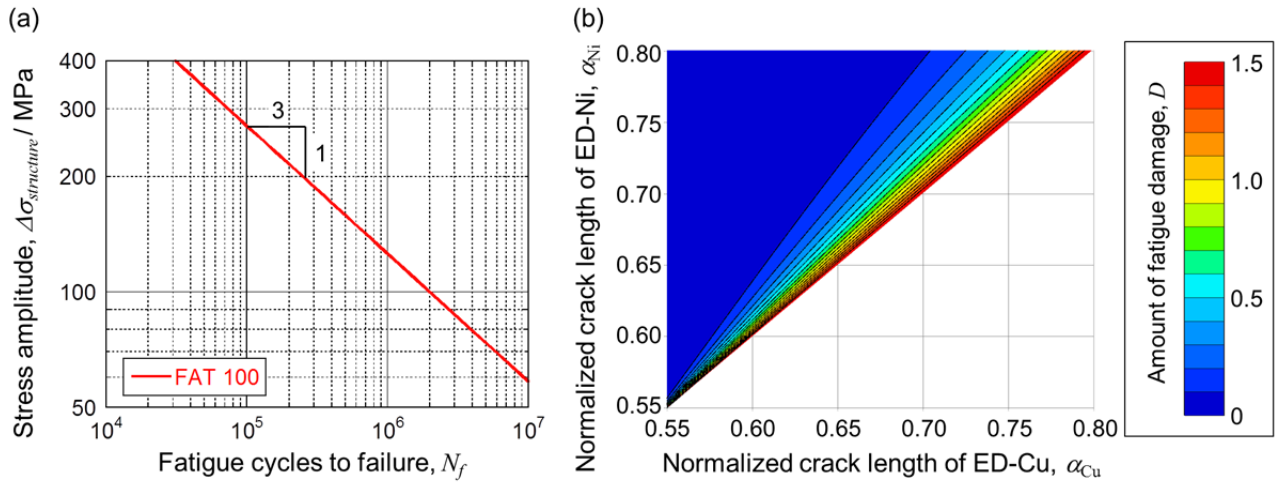

Figure 9. (a) S-N curve of FAT100 (Fatigue strength at two million cycles is 100 MPa), (b) Estimation map of the amount of fatigue damage as a function of normalized crack length in two sensors.

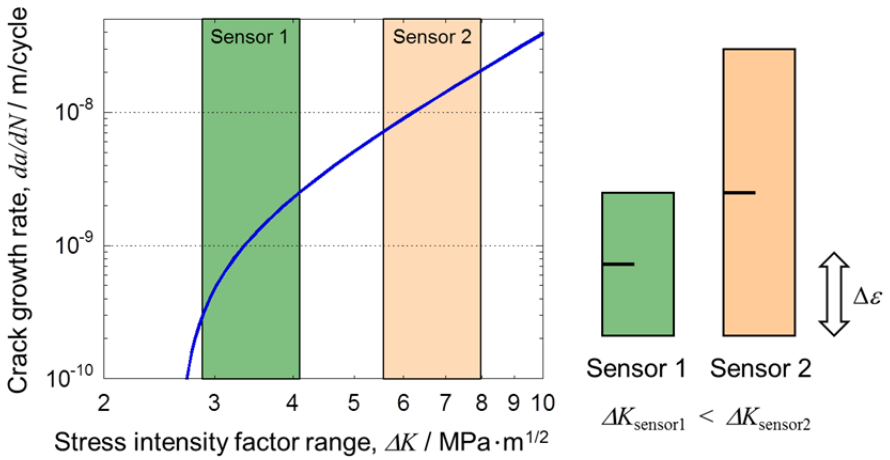

Figure 10. Schematic of estimation method of fatigue damage using single material.

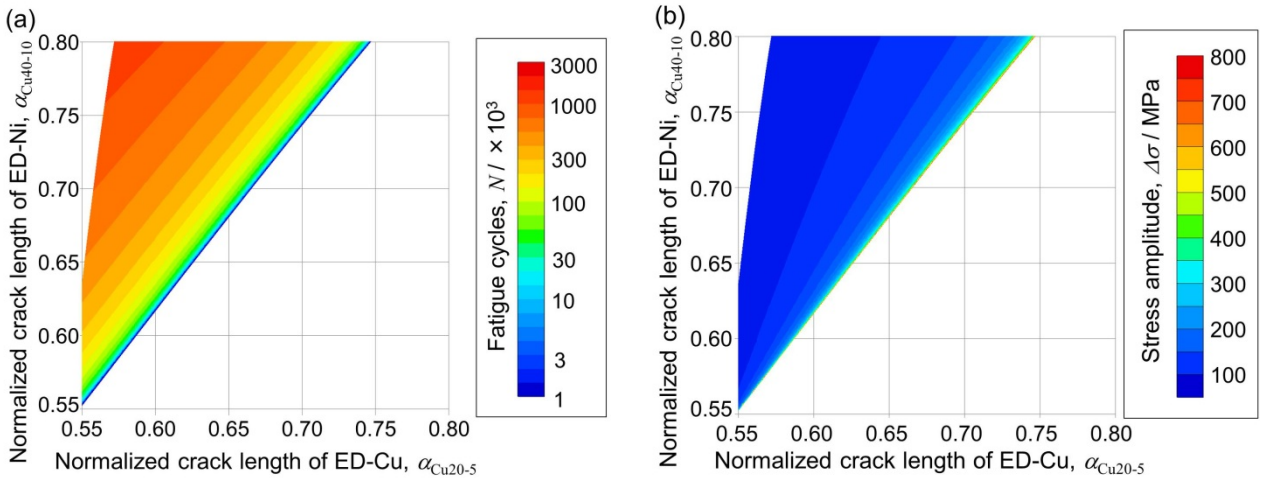

Figure 11. Estimation map of (a) fatigue cycles and (b) stress amplitude of steel structure as a function of normalized crack length in two sensors made of same material.

5. Conclusions

In the present study, near-threshold fatigue crack growth behavior in thin pure copper sheet with pre-crack was evaluated under strain-controlled fatigue testing in order to obtain the sensor characteristics of smart stress-memory patch and the following conclusions were obtained.

(1) Using a function describing the initiation as well as the stable growth of fatigue cracks, relationship between stress intensity factor range and crack growth rate of ED-Cu was successfully fitted to one equation regardless of strain amplitude, strain ration and specimen geometry.

(2) It was shown that the stress amplitude and the cyclic number can be estimated from the crack lengths of two sensors made of ED-Ni and ED-Cu. Furthermore, using S-N curve of structural material, the cumulative fatigue damage could be evaluated as a function of crack length of smart patch.

(3) Based on these experimental results, a new equation for estimating fatigue cycles and stress amplitude from fatigue crack length of two specimens was derived. This equation overcame the limitation that the patch requires two or more materials with different fatigue characteristics.

Acknowledgements

This study was partially supported by research fellowship program (No. 22･10020) of Japan Society for the Promotion of Science (JSPS).

References

[1] S. Nambu, M. Enoki, Scattering in fatigue, crack growth of thin pure copper sheet for smart stress memory patch. ISIJ Int., 47 (2007) 1687-1691.
[2] S. Nambu, M. Enoki, Monitoring of Acoustic Emission Activity of Smart Stress Memory Patch to Estimate Maximum Fatigue Stress for Structural Health Monitoring. ISIJ Int., 51 (2011) 88-92.
[3] T. Shiraiwa, M. Enoki, Evaluation of Fatigue Properties of Steel Bar by Smart Stress-memory Patch. ISIJ Int., 51 (2011) 250-255.
[4] T. Shiraiwa, M. Enoki, Fatigue Crack Length Measurement of Sputtered Metal Film for RFID-based Smart Stress Memory Patch. ISIJ Int., 51 (2011) 1480-1486.
[5] S. Nambu, M. Enoki, Smart stress-memory patch for fatigue damage of structure. Mater. Trans., 48 (2007) 1244-1248.
[6] Y. Fujino, S. Nambu, M. Enoki, AE behavior of smart stress memory patch after variable amplitude loading. Mod. Phys. Lett. B, 22 (2008) 1105-1110.
[7] H. D. Merchant, M. G. Minor, Y. L. Liu, Mechanical Fatigue of Thin Copper Foil. J. Electron. Mater., 28 (1999) 998-1007.
[8] M. Hommel, O. Kraft, E. Arzt, A new method to study cyclic deformation of thin films in tension and compression. J. Mater. Res., 14 (1999) 2373-2376.
[9] M. Judelewicz, H. U. Künzi, N. Merk, B. Ilschner, Microstructural development during fatigue of copper foils 20–100 μm thick. Mater. Sci. Eng. A, 186 (1994) 135-142.
[10] M. Gonzalez, F. Axisa, M. V. Bulcke, D. Brosteaux, B. Vandevelde, J. Vanfleteren, Design of metal interconnects for stretchable electronic circuits. Microelectron. Reliab., 48 (2008) 825-832.
[11] S. Nambu, M. Enoki, Scattering in fatigue crack growth of thin pure copper sheet for smart stress memory patch. ISIJ Int., 47 (2007) 1687-1691.
[12] T. Hanlon, E. D. Tabachnikova, S. Suresh, Fatigue behavior of nanocrystalline metals and alloys. Int. J. Fatigue, 27 (2005) 1147-1158.
[13] P. J. Torvik, On the Determination of Stresses, Displacements, and Stress-Intensity Factors in Edge-Cracked Sheets With Mixed Boundary Conditions. J. Appl. Mech. , 46 (1979) 611-617.
[14] J. Kohout, A new function describing fatigue crack growth curves. International Journal of Fatigue, 21 (1972) 813–821.
[15] M. A. Miner, Cumulative Damage in Fatigue. J. Appl. Mech., 12 (1945) A159-A164.
[16] S. Suresh, Fatigue of Materials, Cambridge University Press, Cambrige, 1998.